






## Article

# The Compound (*E*)-2-Cyano-*N*,3-diphenylacrylamide (JMPR-01): A Potential Drug for Treatment of Inflammatory Diseases

Pablo Rayff da Silva <sup>1,2,3</sup> , Renan Fernandes do Espírito Santo <sup>4,5</sup>, Camila de Oliveira Melo <sup>1,3</sup> , Fábio Emanuel Pachú Cavalcante <sup>2</sup> , Thássia Borges Costa <sup>2</sup>, Yasmim Vilarim Barbosa <sup>2</sup>, Yvnni M. S. de Medeiros e Silva <sup>3</sup>, Natália Ferreira de Sousa <sup>6</sup>, Cristiane Flora Villarreal <sup>4,5</sup> , Ricardo Olímpio de Moura <sup>1,3</sup>  and Vanda Lucia dos Santos <sup>1,2,\*</sup>



**Citation:** da Silva, P.R.; do Espírito Santo, R.F.; Melo, C.d.O.; Pachú Cavalcante, F.E.; Costa, T.B.; Barbosa, Y.V.; e Silva, Y.M.S.d.M.; de Sousa, N.F.; Villarreal, C.F.; de Moura, R.O.; et al. The Compound (*E*)-2-Cyano-*N*,3-diphenylacrylamide (JMPR-01): A Potential Drug for Treatment of Inflammatory Diseases. *Pharmaceutics* **2022**, *14*, 188. <https://doi.org/10.3390/pharmaceutics14010188>

Academic Editors: João Augusto Oshiro Júnior and Arnobio A. da Silva-Junior

Received: 16 December 2021

Accepted: 10 January 2022

Published: 13 January 2022

**Publisher's Note:** MDPI stays neutral with regard to jurisdictional claims in published maps and institutional affiliations.



**Copyright:** © 2022 by the authors. Licensee MDPI, Basel, Switzerland. This article is an open access article distributed under the terms and conditions of the Creative Commons Attribution (CC BY) license (<https://creativecommons.org/licenses/by/4.0/>).

- <sup>1</sup> Programa de Pós Graduação em Ciências Farmacêuticas, Universidade Estadual da Paraíba, Campina Grande 58429-500, PB, Brazil; pablo-rayff@hotmail.com (P.R.d.S.); camillamello-@hotmail.com (C.d.O.M.); ricardo.olimpiodemoura@gmail.com (R.O.d.M.)
- <sup>2</sup> Laboratório de Ensaios Farmacológicos, Departamento de Farmácia, Universidade Estadual da Paraíba, Campina Grande 58429-500, PB, Brazil; fabiocavalcante221@gmail.com (F.E.P.C.); thassiacosta5@gmail.com (T.B.C.); yasmimvilarim.b@gmail.com (Y.V.B.)
- <sup>3</sup> Laboratório de Desenvolvimento e Síntese de Fármacos, Departamento de Farmácia, Universidade Estadual da Paraíba, Campina Grande 58429-500, PB, Brazil; Yvnnim@gmail.com
- <sup>4</sup> Instituto Gonçalo Moniz, Fundação Oswaldo Cruz, Salvador 40296-710, BA, Brazil; r.fernandes88@hotmail.com (R.F.d.E.S.); cfv@ufba.br (C.F.V.)
- <sup>5</sup> Faculdade de Farmácia, Universidade Federal da Bahia, Salvador 40170-290, BA, Brazil
- <sup>6</sup> Programa de Pós Graduação em Produtos Naturais, Sintéticos e Bioativos, Universidade Federal da Paraíba, João Pessoa 58051-900, PB, Brazil; nferreiradesousa.nfs@gmail.com
- \* Correspondence: vandaluciasantos16@gmail.com; Tel.: +55-83-9-8846-6949

**Abstract:** The compound (*E*)-2-cyano-*N*,3-diphenylacrylamide (JMPR-01) was structurally developed using bioisosteric modifications of a hybrid prototype as formed from fragments of indomethacin and paracetamol. Initially, in vitro assays were performed to determine cell viability (in macrophage cultures), and its ability to modulate the synthesis of nitrite and cytokines (IL-1 $\beta$  and TNF $\alpha$ ) in non-cytotoxic concentrations. In vivo, anti-inflammatory activity was explored using the CFA-induced paw edema and zymosan-induced peritonitis models. To investigate possible molecular targets, molecular docking was performed with the following crystallographic structures: LT-A4-H, PDE4B, COX-2, 5-LOX, and iNOS. As results, we observed a significant reduction in the production of nitrite and IL-1 $\beta$  at all concentrations used, and also for TNF $\alpha$  with JMPR-01 at 50 and 25  $\mu$ M. The anti-edematogenic activity of JMPR-01 (100 mg/kg) was significant, reducing edema at 2–6 h, similar to the dexamethasone control. In induced peritonitis, JMPR-01 reduced leukocyte migration by 61.8, 68.5, and 90.5% at respective doses of 5, 10, and 50 mg/kg. In silico, JMPR-01 presented satisfactory coupling; mainly with LT-A4-H, PDE4B, and iNOS. These preliminary results demonstrate the strong potential of JMPR-01 to become a drug for the treatment of inflammatory diseases.

**Keywords:** bioisosterism; phenylacrylamide; immunomodulation; inflammation

## 1. Introduction

Inflammation is the body's reaction to aggressive chemical, physical, or biological agents, promoting coordinated activation of signaling pathways with the aim of instituting repair processes. The process is initiated by activation of standard cell surface receptors, which recognize stimuli, and activate intracellular signaling cascades, inducing the translocation of transcription factors and resulting in the expression of various inflammatory mediators [1,2]. At the tissue level, during the inflammatory response, typical acute symptoms such as edema, redness, heat, and pain, which may progress to loss of tissue function, are observed [3,4].

An acute process, if unresolved, can become both chronic and part of disease pathogenesis. According to the World Health Organization (WHO), inflammatory diseases are the third leading cause of death, accounting for about 3.46 million deaths, corresponding to 10.8% of the world total [5]. According to Global Business Intelligence Research, Non-steroidal anti-inflammatory drugs (NSAIDs) and steroids constitute one of the main classes of drugs used worldwide, mobilizing USD 85.9 billion in 2017 [6].

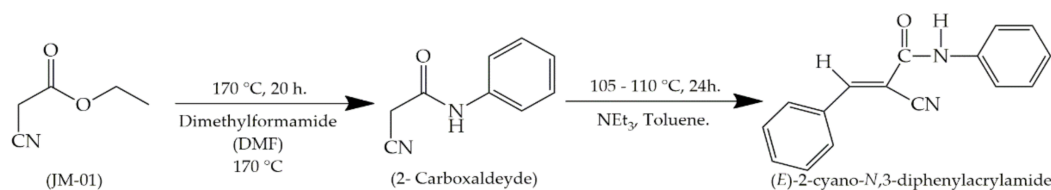
Many classes of drugs, such as non-steroidal anti-inflammatory drugs (NSAIDs) and corticosteroids have been shown to be effective in the treatment of inflammatory disorders [5,7]. However, when used for prolonged periods or in non-therapeutic doses, these agents can promote gastrointestinal, renal, and liver disorders, and in the case of steroids, immunosuppression and metabolic changes. Research for new clinically acceptable compounds and bioactive molecules against inflammation is therefore a continuing demand.

As for the development of promising drugs with anti-inflammatory potential, medicinal chemistry has become an important tool in planning new molecules with therapeutic potential, aimed at maintaining pharmacological response and with better toxicity profiles than previously described for conventional anti-inflammatory drugs. In this context, new structures are synthesized using privileged carbon skeletons as a basis, such as the phenylacrylamide function. Our research aimed to synthesize and investigate the anti-inflammatory potential of (*E*)-2-cyano-*N*,3-diphenylacrylamide, obtained by organic synthesis from bioisosteric modifications of a previously studied drug [8] and resulting from the hybridization of molecular fragments of the anti-inflammatory drugs indomethacin and paracetamol.

## 2. Materials and Methods

### 2.1. General Procedure for the Synthesis of Compound (*E*)-2-Cyano-*N*,3-diphenylacrylamide (JMPR-01)

To obtain the JMPR-01, the following products were used in equimolar (1 mmol): 2-cyano-*N*-phenylacetamide (JM-01), previously synthesized; and 2-carboxyaldehyde (Sigma-Aldrich, St. Louis, MO, USA). Toluene (10 mL) (Vetec, Rio de Janeiro, Brazil) was used as reaction medium, added with 5–10 drops of the catalyst, triethylamine (Sigma-Aldrich, St. Louis, MO, USA) (Scheme 1). The reaction was kept under magnetic stirring, for 24 h at a temperature between 105–110 °C, and its end was observed by Analytical Thin Chromatography (CCDA). The reaction was filtered and the obtained crystals were washed with ice-cold distilled water, and then recrystallized in ethanol–water 1:1. The product was then analyzed by <sup>1</sup>H and <sup>13</sup>C NMR (Agilent NMR spectrometer, model Mercury Plus 500 MHz, OXFORD 300 magneto-NMR), infrared spectroscopy (IRPrestige-21 Spectrophotometer) and mass spectrometry (Shimadzu® AXIMA series MALDI-TOF/MS).



**Scheme 1.** Synthesis of (*E*)-2-cyano-*N*,3-diphenylacrylamide—JMPR-01.

### 2.2. Physical-Chemical Properties and Spectroscopic Data of (*E*)-2-Cyano-*N*,3-diphenylacrylamide (JMPR-01)

JMPR-01 was obtained as gray powder (72.37%). M.p. (°C): 200,26. R<sub>f</sub> (7:3 AcOEt/n-hexane): 0.60. IR (ATR): 1596 (NH, amide folding), 1682 (C=O), 2227 (CN), 3317 (NH, secondary amide stretch), 3053 (=C-H), 1531–1440 (C=C, Ar) cm<sup>-1</sup>. NMR <sup>1</sup>H (500 MHz, DMSO-d<sub>6</sub>): 10.43 (1H, s, NH amide); 8.30 (1H, s, C=CH); 8.05–7.96 (2H, m, Ar phenylacetamide); 7.72–7.66 (2H, m, Ar phenylacetamide); 7.39 (2H, t, J = 7.9 Hz, Ar phenylacetamide) 7.67–7.57 (3H, m, Ar phenylacetamide); 7.19–7.12 (2H, m, Ar phenylacetamide).



NMR de  $^{13}\text{C}$  (124 MHz, DMSO-d<sub>6</sub>):  $\delta$  160.97 (C, C=O); 151.27 138.68 (C, N-Ar phenylacetamide), 132.94, (C, Ar phenylacetamide), 132.37 (C, Ar phenylacetamide), 130.52 (C, Ar phenylacetamide), 129.77 (C, Ar phenylacetamide) 129.24 (C, Ar phenylacetamide), 124.84 (C, Ar phenylacetamide), 121.02 (C, Ar phenylacetamide), 116.68 (C, CN), 107.81 (C, adjacent to CN). HRMS  $m/z$  [M + H]<sup>+</sup> calculated for C<sub>16</sub> H<sub>12</sub>N<sub>2</sub>O; 248.09 found: 249.01.

### 2.3. Thermal Characterization

#### 2.3.1. Differential Scanning Calorimetry (DSC)

The Differential Scanning Calorimetry curve was obtained in a differential exploratory module of the Q20 (TA<sup>®</sup>—Instruments, New Castle, DE, USA). Samples of  $2.00 \pm 0.05$  mg were used, placed in hermetically sealed aluminum crucibles, analyzed at a heating ratio of  $10\text{ }^\circ\text{C min}^{-1}$  with a temperature of  $25\text{ }^\circ\text{C}$  to  $400\text{ }^\circ\text{C}$ , under a nitrogen atmosphere with flow  $50\text{ mL min}^{-1}$ .

#### 2.3.2. Thermogravimetric (TG)

The thermogravimetric curve of JMPR-01 was obtained in a Pyris 1 TGA (Perkin Elmer<sup>®</sup>, Boston, MA, USA) thermal analyzer using alumina crucibles with  $8 \pm 0.1$  mg samples, under nitrogen atmosphere at a  $50\text{ mL min}^{-1}$  flow rate. The experiments were carried out in the temperature range of  $25\text{--}900\text{ }^\circ\text{C}$ , with a heating rate of  $10\text{ }^\circ\text{C min}^{-1}$ .

### 2.4. Biological Activity

#### 2.4.1. Macrophages Cytotoxicity

The cytotoxicity of JMPR-01 was determined using the cell line J774 according to the methodology proposed by Mosmann (1983) [9], adapted according to Espirito-Santo (2017) [10]. Macrophages were seeded in 96-well plates ( $2 \times 10^5$  cells/well) in Dulbecco's Modified Eagle Medium (DMEM; Life Technologies<sup>®</sup>, Gibco BRL<sup>®</sup>, Gaithersburg, MD, USA), supplemented with 10% fetal bovine serum (Gibco BRL<sup>®</sup>, Gaithersburg, MD, USA) and  $50\text{ }\mu\text{g/mL}$  of gentamicin (Novafarma, Anápolis, GO, Brazil). Afterwards, the plates were incubated for 2 h at  $37^\circ$  in an atmosphere of 5% CO<sub>2</sub>. The test molecule was added to the wells in triplicate at concentrations of 100, 50, 25, 12.5 and  $6.25\text{ }\mu\text{M}$ , and incubated again for 72 h. As a positive control,  $10\text{ }\mu\text{M}$  gentian violet (Synth, São Paulo, Brazil) was used. Finally,  $20\text{ }\mu\text{L/well}$  of Alamarblue Cell Viability Reagent (Invitrogen<sup>®</sup>, Carlsbad, CA, USA) was added to the plate, holding for 12 h. Colorimetric scanning was performed at a length from 570 to 600 nm.

#### 2.4.2. Assessment of Cytokine and Nitric Oxide Production by Macrophages

To determine the influence of JMPR-01 on cytokines and nitric oxide (NO), J774 macrophages were seeded in 96-well culture plates at a concentration of  $2 \times 10^5$  cells per well in DMEM medium supplemented with 10% FBS and  $50\text{ }\mu\text{g/mL}$  of gentamicin for 2 h at  $37\text{ }^\circ\text{C}$  under an atmosphere of 5% CO<sub>2</sub>. After seeding, the cells were treated with the molecule, at non-cytotoxic concentrations, with the vehicle (negative control) and with dexamethasone  $40\text{ }\mu\text{M}$  (positive control), and then stimulated with LPS ( $500\text{ ng/mL}$ , Sigma, St. Louis, MO, USA) and IFN- $\gamma$  ( $5\text{ ng/mL}$ ; Sigma, St. Louis, MO, USA) and incubated at  $37\text{ }^\circ\text{C}$ . After an incubation period of 4 h (to measure TNF- $\alpha$ ) and 24 h (to quantify IL-1 $\beta$  and nitrite), cell supernatants were collected, and kept at  $-80\text{ }^\circ\text{C}$ . Then, cytokine concentrations were determined by enzyme-linked immunosorbent assay (ELISA), using the DuoSet kit from R & D Systems (Minneapolis, MN, USA). The quantification of nitric oxide was performed using the Griess method according to Green et al. (1982) [11].

#### 2.4.3. Animals

Adult male Swiss Webster mice weighing between 25 and 35 g, obtained from the Prof. Eduardo Barbosa Beserra Animal Facilities at the Paraíba State University and the Gonçalo Moniz Institute (FIOCRUZ; Salvador, Brazil), were used. In the vivarium, the animals were kept in plastic cages, under room temperature and humidity ( $23 \pm 2\text{ }^\circ\text{C}$ ),

with a 12 h light-dark cycle, and fed with feed and water ad libitum. All studies were performed between 08:00 and 17:00 p.m. The animal care and handling procedures were followed in strict accordance with the recommendations of the Guide for the Care and Use of Laboratory Animals of the National Institutes of Health and the Brazilian College of Animal Experimentation. Previously, the project was approved by the Ethics Committee on Animal Use under number 003/2021. All procedures from the beginning of the study until the time of euthanasia were performed to avoid suffering and reduce the discomfort and pain of the animals.

#### 2.4.4. Inflammatory Model

##### Zymosan-Induced Acute Peritonitis in Mice

Mice were divided into groups: positive control, negative control and test groups, which were treated orally with saline (5% DMSO), indomethacin 10 mg/kg and JMPR-01 at doses of 5, 10 and 50 mg/kg, respectively. After 1 h of the treatments, 0.25 mL of 2% zymosan was injected intraperitoneally. Four hours after induction of inflammation, the animals were euthanized by administering 2 mL of heparinized phosphate-buffered saline into the intraperitoneal cavity [12,13]. At the end, an incision was made, collecting the exudate, whose cells were resuspended in 500  $\mu$ L of PBS and 10  $\mu$ L of Turk's fluid (1:20). To count the leukocytes, a Neubauer chamber was used under light microscopy, examining the four external quadrants.

##### Plethysmometer Test

Mice were lightly anesthetized with halothane and received an intraplantar injection of complete Freund's adjuvant (CFA) (Sigma) in the right paw in a final volume of 20  $\mu$ L, according to previously reported method [14]. JMPR-01 (50 and 100 mg/kg) or vehicle (5% DMSO in saline; control group) was administered by p.o. route 40 min before phlogiston agent. Dexamethasone (2 mg/kg, i.p) was used as standard. The paw volume was assessed ( $\text{mm}^3$ ) by plethysmometer (Ugo Basile, Comerio, Italy) as described above. The amount of paw swelling was determined for each mouse and data were represented as paw volume variation ( $\Delta$ ,  $\text{mm}^3$ ).

#### 2.5. Docking Studies

The structure of the JMPR-01 was built with Chemdraw professional 3D 15.0 software, optimized by a minimization of the molecular energy using molecular mechanics (MM2) and then saved as MOL2 files. With the use of AutoDockTools-1.5.6, non-polar hydrogens were merged with the corresponding carbons, and then partial charges of atoms were calculated using the Gasteiger procedure implemented in the AutoDockTools package. Finally, the rotatable bonds of the ligands were defined, the structures were saved as pdbqt and used for docking studies.

The crystal structures of Inducible nitric oxide synthase (PDB ID: 3E7G), Phosphodiesterase 4B (PDB ID: 1XMU), Leukotriene A4 hydrolase (PDB ID: 1HS6), 5-Lipoxygenase (PDB ID: 6NCF) and Cyclooxygenase-2 (PDB ID: 3LN1) were retrieved from RCSB Protein Data Bank as described [15,16]. With the use of Molecular Graphics System, PyMOL, water molecules and other heteroatoms were removed. Then, using AutoDockTools, non-polar hydrogens were merged, and polar hydrogens added to the structures of the proteins. Kollman charges were added and the structures were saved as pdbqt for the docking studies.

The Lamarckian genetic algorithm in AutoDock 4.2.6 was applied to search the best conformation and orientation of the ligands. The global optimization was started with a population of 150 randomly positioned individuals with a maximum of 2,500,000 energy evaluations and a maximum of 27,000 generations. During each docking experiment, 100 runs were carried out. The resulting docking poses were analyzed using AutoDockTools and Discovery Studio Visualizer 2021 Client. To validate the docking procedure, the co-crystallized ligand was previously docked to the protein, obtaining a RMSD value of  $\leq 2$  Å in the redocking procedure.

## 2.6. Statistical Analysis

Data are presented as means  $\pm$  SEM of measurements made on 6 animals in each group. Comparisons across three or more treatments were made using one-way ANOVA with Tukey's post hoc test or repeated measures two-way ANOVA with Bonferroni's post hoc test, when appropriate. All data were analyzed using the Prism 5.01 computer software (GraphPad, San Diego, CA, USA). Statistical differences were considered to be significant at  $p < 0.05$ .

## 3. Results

### 3.1. Synthesis

The intermediate 2-cyano-N-phenylacetamide (JM-01) (previously synthesized and characterized by Silva (2018) was used to synthesize the phenylacrylamide derivative 2-cyano-N-3-diphenylacrylamide (JM-PR-01). The final molecule was obtained through the *Knoevenagel* condensation reaction presented in Scheme 1. The *Knoevenagel* condensation is an important organic reaction in the formation of a carbon–carbon double bond between the carbonyl function and activated methylene groups. Many  $\alpha$ ,  $\beta$ -unsaturated products obtained by this type of condensation have been widely used as intermediates in the synthesis of drugs, chemicals, cosmetics, foodstuffs, and agrochemicals [17–19].

Due to its aprotic nature which favors catalytic activity at higher temperatures, toluene was used as a reaction medium. The catalyst used was triethylamine (NEt<sub>3</sub>), whose function in the reaction medium was to abstract a carbon proton directly linked to nitrile and carbonyl, which, due to a negative mesomeric effect, is deficient in electrons acquiring a partially positive charge. The electronic effect exerted by the ligands makes the hydrogen more acidic, facilitating the loss of the proton to form the carbanion. *Knoevenagel* condensation results from the nucleophilic attack of the carbanion on the carbonyl group of the aldehyde, due to its electron-deficient nature. Protonated triethylamine transfers its proton to the oxygen of the aldehyde, forms a hydroxyl, and restores the base.

The reaction's completion is characterized by protonation of the hydroxyl and its full exit in the form of water. This process allows the carbon to oxidize and results in the formation of a double bond. After synthesis of JM-PR-01, spectroscopic and spectrometric methods were performed for its structural elucidation and determination of physicochemical parameters: theoretical partition coefficient (LogP), molar mass (MM) (Chemdraw), retention factor (Rf), and yield, shown in Table 1.

**Table 1.** Physicochemical characteristic of the phenylacrylamide derivative JM-PR-01.

Molecule	Appearance	MM (g/mol)	Yield (%)	Rf <sup>1</sup>	FM *	Log (P)
JM-PR-01	Gray powder	248.09	72.37	0.60 <sup>1</sup>	C <sub>16</sub> H <sub>12</sub> N <sub>2</sub> O	2.43

\* MF = Molecular formula; <sup>1</sup> Rf: hexane/AcOEt 7:3 system.

### 3.2. Structural Elucidation

Through <sup>1</sup>H NMR analysis, it was possible to identify a singlet referring to the NH group of the amide that were detected with displacement at  $\delta$  10.43 ppm. This signal is outside the characteristic range of 5.0 to 9.0 ppm due to the anisotropic effect, which leaves the H less shielded. It was observed peaks characteristic of singlet (s) at  $\delta$  8.30 ppm indicative of condensation between the aldehyde and methylene group, culminating in the formation of the vinyl group (C=CH). Other aromatic hydrogens could be found with displacements ranging between  $\delta$  7.12 to 8.05 in triplet (t) and multiplet (m) form. The <sup>13</sup>C NMR spectrum also confirmed the structure by the presence of signals correspondent to the compound. Two signals were observed in the negative region at 160.97 and 138.68 ppm, corresponding respectively to the carbonyl carbon and the quaternary carbon, and indicating *Knoevenagel* condensation. Likewise, it was possible to detect signals at 151.27 ppm, indicative of vinyl carbons, and at 116.68 ppm, which is diagnostic of the nitrile function. Infrared results also assisted in the structural characterization of the JM-PR-01. The follow-

ing bands were observed: 1682, 2227, and 3017  $\text{cm}^{-1}$ , characteristic of elongation of the carbonyl, nitrile, and amide groups, respectively. Ultimately, mass spectrometry (MS) was useful to confirm the structure of the novel synthesized compound, exhibiting the result of  $m/z = 249.10$  (Spectroscopic and spectrometric data can be found in the Supplementary Materials, Figures S1–S4).

### 3.3. Thermal Characterization (DSC and TGA)

The DSC curve for JMPR-01 presents a well-defined endothermic peak, characteristic of melting, occurring at a temperature of 200.26  $^{\circ}\text{C}$  ( $\Delta H = 222.5 \text{ J g}^{-1}$ ) and a purity of 99.82%. Regarding the thermogravimetric curve, we observed a single stage of degradation between 174.35–319.92  $^{\circ}\text{C}$  with a mass loss of 96.74%. At the end of the analysis, the presence of inorganic residues (0.3545%) was verified which did not entirely decompose until 900  $^{\circ}\text{C}$  (The DSC and TGA curves are found in the Supplementary Materials, Figure S5).

## 4. Biological Activity

### 4.1. In Vitro Tests

The anti-inflammatory and immunomodulatory potential of JMPR-01 was explored in a series of cell culture assays using J774 murine macrophages. The first test performed was cell viability using the Alamarblue method, which indicates impairment of cell metabolism through color change by mitochondrial enzymes [20]. For this test, JMPR-01 was used at concentrations of 6.25, 12.5, 25, 50, and 100  $\mu\text{M}$ , as shown in Figure 1. Based on the results, induction of cytotoxic effects occurred at a concentration of 100  $\mu\text{M}$ . Determining the cytotoxic concentration is important, since it allows targeting concentrations of JMPR-01 for use in other tests, such as dosing for nitrite and cytokines. For these tests, concentrations of up to 50  $\mu\text{M}$  were tested, with no changes in cell viability after 72 h.

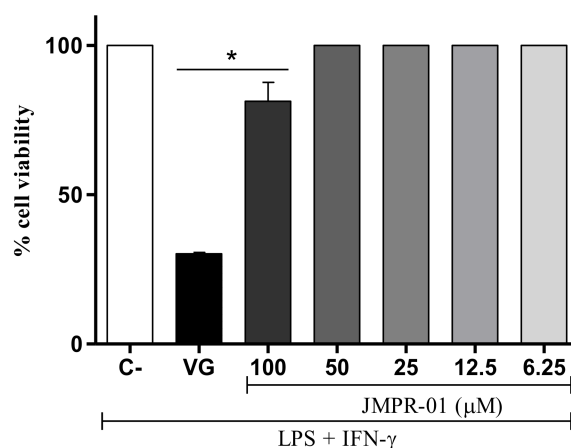


**Figure 1.** In vitro cytotoxicity of J774 macrophage cell treated with JMPR-01 (6.25–100  $\mu\text{M}$ ). The graph represents cell viability at 72 h determined by Alamar Blue assay. Data represents mean standard error of the mean  $\pm$  SEMs;  $n = 4$  determinations per group. \* Significantly different from the vehicle treated cultures ( $p < 0.05$ ); ANOVA followed by Tukey's multiple comparison test.

Macrophages are a principal cell of the immune system, which, when activated by microbial products (such as LPS and  $\text{IFN-}\gamma$ ), produce mediators such as nitric oxide, proteolytic enzymes, and inflammatory cytokines, among others. These substances are part of the pathophysiological inflammation process promoted in tissue and vascular injury [21]. Nitrite is a decomposition product of nitric oxide, important in the cell oxidation process, and quantified in cultures of stimulated macrophages. In Figure 2, JMPR-01 at concentrations of 50–3.125  $\mu\text{M}$  promoted a significant reduction ( $p < 0.05$ ) in nitrite production compared to the un-stimulated control group. Dexamethasone (40  $\mu\text{M}$ ) was used as a standard.



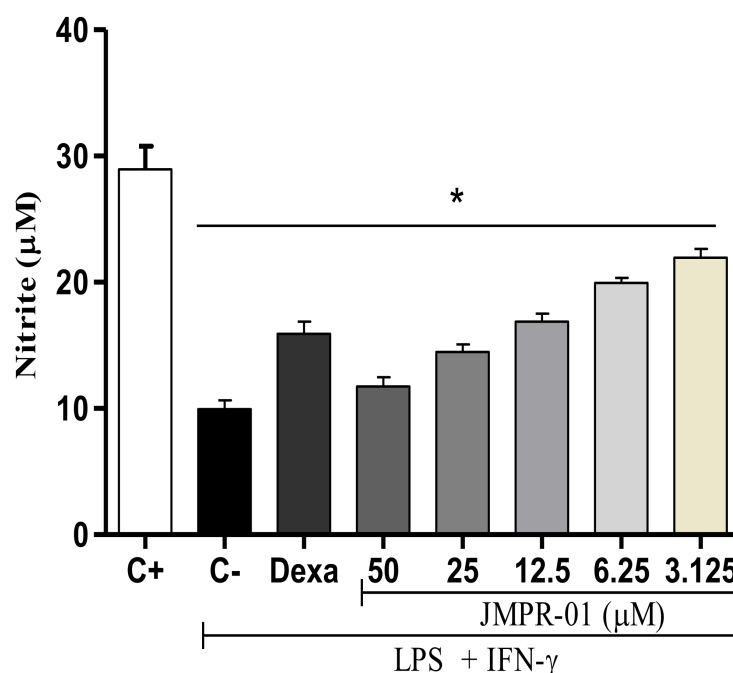


**Figure 2.** Modulation of nitric oxide (NO) (nitrite in  $\mu\text{M}$ ) in activated J774 macrophage cells treated with JMPR-01 (3.125–50  $\mu\text{M}$ ) by the Griess method. Data represents mean standard error of the mean  $\pm$  SEMs;  $n = 6$  determinations per group. \* Significantly different from the vehicle treated cultures stimulated with LPS + IFN- $\gamma$  ( $p < 0.05$ ). ANOVA followed by Tukey's multiple comparison test.

Nitric oxide (NO) is a gas molecule which, when crossing biological membranes, produces reactive species through association with oxygen and superoxides. Its production involves nitric oxide synthase (NOS) enzymes, which are presented in three isoforms: neuronal (nNOS), endothelial (eNOS), and inducible (iNOS), using L-arginine, NADPH, and oxygen as substrates. The inducible form (iNOS) is expressed in the highest concentration in response to inflammatory stress, producing higher concentrations of nitric oxide. In macrophages, iNOS can be induced by LPS, a microbial product. NO promotes the release of leukocytes, macrophages, mast cells, endothelial cells, and platelets. NO also promotes blood flow modulation, leukocyte adhesion to vascular endothelium, and the activity of numerous enzymes which impact inflammatory responses [22,23].

The capacity of JMPR-01 to suppress production of cytokines expressed by macrophage stimulation (interleukin 1 beta (IL-1 $\beta$ ) and tumor necrosis factor alpha (TNF- $\alpha$ )) was also evaluated. Based on the results, there was a significant reduction ( $p < 0.05$ ) of TNF- $\alpha$  after the treatment of cultures with JMPR-01 at concentrations of 50 and 25  $\mu\text{M}$  (Figure 3A). For IL-1 $\beta$ , JMPR-01 inhibited TNF- $\alpha$  at all concentrations (50 to 3.125  $\mu\text{M}$ ) (Figure 3B), which demonstrates its pharmacological potential even at its lowest tested concentration. Dexamethasone at a concentration of 40  $\mu\text{M}$  was used as the standard drug for this assay as well.

From the dose-response curve of JMPR-01, standardized by TNF- $\alpha$  inhibition in J774 macrophage cultures, the CC50, EC50 and Selectivity Index (S.I.) values were obtained. The cytotoxic concentration that reduced cell viability by 50% compared to the control group was  $977.25 \pm 655.36 \mu\text{M}$ . The concentration of the compound for which 50% of the effect was observed was  $7.02 \pm 4.24 \mu\text{M}$ . From the ratio (CC50/EC50) was determined (S.I.), which showed a value of 139.20 (Table S1 in the Supplementary Materials). Given these results, JMPR-01 proves to be a strong candidate as an anti-inflammatory agent, encouraging subsequent in vivo assays.

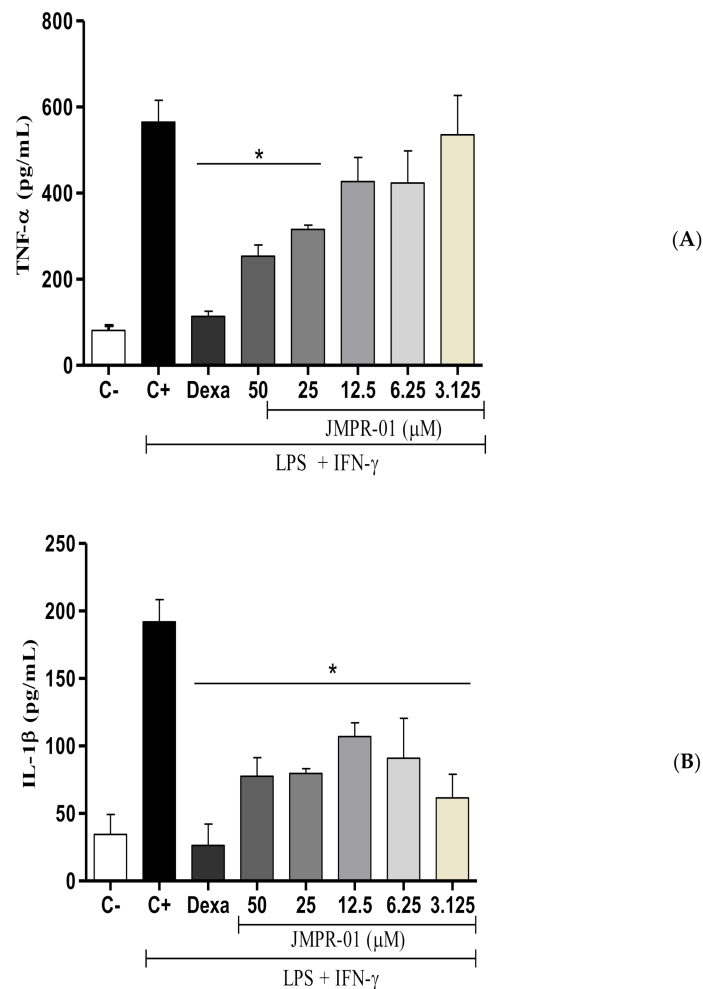


**Figure 3.** Inhibition of cytokines TNF- $\alpha$  (A) and IL-1 $\beta$  (B) in activated J774 macrophage cells treated with JMPR-01 (3.125–50  $\mu$ M) by enzyme-linked immunosorbent assay (ELISA). Data represents mean standard error of the mean  $\pm$  SEMs;  $n = 4$  for TNF- $\alpha$  and  $n = 6$  IL-1 $\beta$  determinations per group. \* Significantly different from the vehicle treated cultures stimulated with LPS + IFN- $\gamma$  ( $p < 0.05$ ). ANOVA followed by Tukey's multiple comparison test.

Based on the observed reduced expression of TNF- $\alpha$ , IL-1 $\beta$ , and nitrite *in vitro*, it can be inferred that a regulatory mechanism is correlated with this transcriptional pathway effect, including a possible decrease in oxidative stress, and inhibition of key regulators of the NF- $\kappa$ B pathway. There are few studies evaluating the performance of phenylacrylamide derivatives in this effect, but they do suggest that their Michael acceptor regions bind to cysteine residues in Keap-1 cytosolic proteins, which act as redox sensors and negative regulators of Nrf2 (nuclear factor erythroid 2 related factor 2), activating the expression of antioxidant and anti-inflammatory enzymes [24–26]. Our results suggest possible mechanisms of action of phenylacrylamide derivatives towards the inhibition of inflammatory mediators involved in inflammatory signaling, and allow for the future development of promising drugs to treat inflammatory diseases.

#### 4.2. *In Vivo* Tests

##### 4.2.1. Peritonitis Induced Zymosan

Leukocyte recruitment involves intercellular communication between endothelium and defense cells, forming the leukocyte adhesion cascade. Subsequent phases involve the release of inflammatory mediators into the vessel lumen, activation of resident cells, and leukocyte chemotaxis towards the inflammation site [27,28]. An *in vivo* peritonitis assay

was used to investigate the anti-inflammatory pharmacology and potential of the test drug to decrease leukocyte migration.

Zymosan (obtained from the polysaccharide wall of the fungus *Saccharomyces cerevisiae*) was used as a phlogiston agent [29]. Its action occurs through activation of components of the inflammatory machinery, such as complement system proteins, prostaglandins, leukotrienes, ROS, and platelet aggregation factor [30]. Through direct macrophage stimulation mediated by Toll-like TLR-2 and TLR6 receptors, it was observed that Zymosan was able to induce phagocytosis and the production of inflammatory mediators such as TNF- $\alpha$ , IL-1 $\beta$ , by activating the NF- $\kappa$ B pathway [31].

As can be seen in Figure 4 of the peritonitis model, JMPR-01 significantly ( $p < 0.05$ ) inhibited leukocyte migration by 61.8, 68.5, and 90.5%, at respective doses of 5, 10, and 50 mg/kg. For the group treated with the standard indomethacin (10 mg/kg), inhibition was 45%. All groups were compared to control (DMSO 5% + saline).

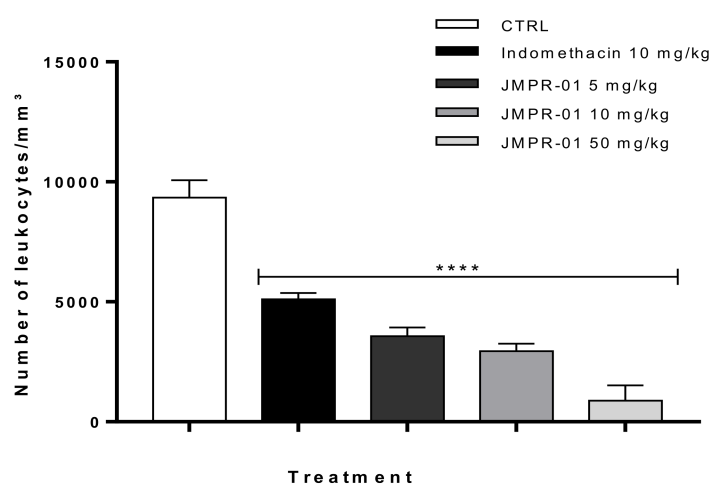


**Figure 4.** Influence of JMPR-01 (5, 10 and 50 mg/kg) treatment on total leukocyte count in the peritonitis induced by zymosan. Data are expressed as means  $\pm$  SEMs;  $n = 6$  mice per group. Two-way ANOVA followed by the Bonferroni's test. \*\*\*\* ( $p < 0.0001$ ) significantly different from the control group.

Studies involving Zymosan-induced peritonitis reveal that in the initial phase of administration, animals present vascular permeability and increased levels of myeloperoxidase, demonstrating massive activity involving recruitment and activation of leukocytes [31,32]. In the inflammatory process, leukocyte chemotaxis involves marginalization, capture, rollover, activation, adhesion, and transmigration to the inflammation center [33]. Depending on the microenvironment where inflammation occurs, these processes include different signaling pathways and chemo-attractants [34]. These data corroborate in vitro human umbilical vein endothelial cell studies, where it was observed that IL1- $\beta$  and TNF- $\alpha$  mediate eosinophil adhesion and trans-endothelial migration, stimulating the release of ICAM-1 (intercellular adhesion molecule-1) E-selectin, and VCAM-1 (vascular cell adhesion molecule-1) [35].

#### 4.2.2. Paw Edema

Vascular responses are the first changes seen in the inflammatory cascade. They involve vasodilation, hyperemia, and increased vascular permeability, to enable the flow of proteins, electrolytes, and exudate into the interstitium [36]. Vascular responses are mediated directly or indirectly by chemical factors caused by inflammatory stimulus in plasma cells and proteins, resulting in what can be seen clinically as edema [37].

Complete Freund's Adjuvant (CFA) consists of inactivated *Mycobacterium tuberculosis* and mineral oil. It is an inducer of inflammatory processes, acting through mobilization

and activation of antigen-presenting cells (APCs), and increasing the response of T cells [38]. In addition to immunological manifestations, CFA can trigger the release of inflammatory mediators such as PGE2, NO, leukotriene B4 (LTB4), TNF- $\alpha$ , IL-2, and IL-17 [39].

According to Ben et al. [40] and Gris et al. [41] in models of rheumatoid arthritis and nociception, CFA is commonly used [38,42] in experimental inflammation models as an inducing agent, having shown that it induces a chronic inflammatory response after intraplantar administration edema with a peak within 24 h occurs.

Figure 5 presents the results of evaluation of JMPR-01 anti-inflammatory activity in the CFA-induced paw edema model. Pre-treatment carried out with JMPR-01 at a dose of 50 mg/kg inhibited formation of edema from 6 h onwards, with activity ceasing by 24 h. Using the compound in a higher dose (100 mg/kg), a satisfactory inhibition was observed from 2 to 6 h, with similar activity to the Dexamethasone control, yet without being significantly maintained after 24 h.

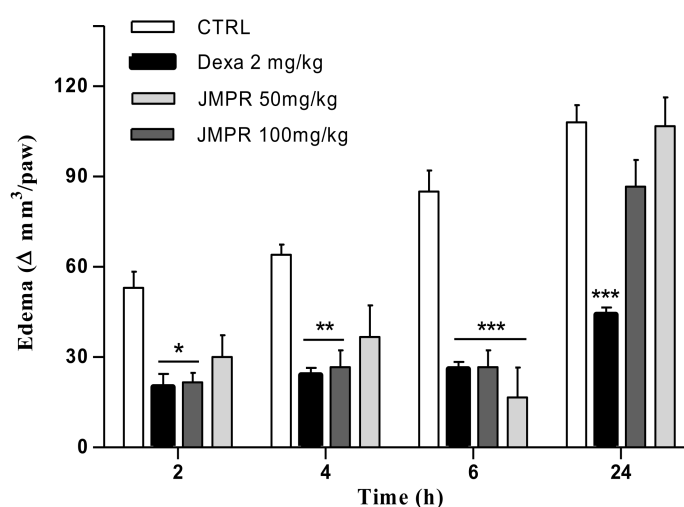


**Figure 5.** Influence of JMPR-01 (50 and 100 mg/kg) in the CFA-induced paw edema. Paw edema was measured 2, 4, 6 and 24 h after CFA, represented as paw volume variation. Data are expressed as means  $\pm$  SEMs;  $n = 6$  mice per group. Two-way ANOVA followed by the Bonferroni's test. \* ( $p < 0.05$ ), \*\* ( $p < 0.01$ ) and \*\*\* ( $p < 0.001$ ) significantly different from the control group.

In vitro, JMPR-01 was shown to suppress TNF- $\alpha$  and IL-1 $\beta$  production by macrophages stimulated with LPS and IFN- $\gamma$ ; making it plausible that this effect may contribute to the anti-edema activity obtained. This assumption is based on modulation (by TNF- $\alpha$  and IL-1 $\beta$ ) of gene expression responsible for encoding the iNOS enzyme, through the p38 MAPK pathway and activation of the nuclear factor kappa-B (NF- $\kappa$ B) [42,43], as well as the significant reduction in nitrite production (a metabolite used to measure NO in vitro). Once expressed, iNOS catalyzes synthesis of NO, (a molecule with a stimulating action on the soluble guanylate cyclase enzyme (sGC) with consequent formation of cyclic guanosine monophosphate (cGMP)—especially in this context, due to its vasodilator activity) [44]. With the *Zymosan*-induced paw edema test being nonspecific, the action of JMPR-01 may result from inhibition of many mediators that contribute to edema promoting activity. These in silico results may contribute to predict its behavior in important targets for anti-inflammatory activity.

#### 4.3. Docking Studies

In silico studies use molecular docking to predict the most favorable conformation, and orientation or “pose” assumed by a ligand, as well as the interactions established between molecules and biological targets. Consequently, molecular docking allows elucidation of fundamental biochemical processes through characterization of the behavior of small molecules when inserted in the active site [45,46].





in addition to the maintenance of vascular tone and permeability, (as suggested in the present paw edema model in this study, and as well as the affinity of the tested compound for iNOS) is related to the observed in vitro modulation of nitrite production [37,50].

Figure 7 presents JMPR-01 and the AR-C95791 ligand—iNOS target interactions; it is noteworthy that JMPR-01 established additional interactions with the amino acid residues Gln 263 and Glu 377, justifying greater affinity with the active site. According to Garcin et al. (2008), [51] these residues are essential for the inhibitory activity of this target, since substitutions resulted in binding affinity reductions (Kd), especially in relation to residue Glu 377, whose Kd ranged from 0.4  $\mu$ M to above 100  $\mu$ M. In addition to having interactions with residues in common (Val 352 and Pro 350) with the co-crystallized target inhibitor IC<sub>50</sub> = 0.35  $\mu$ M—iNOS isoenzyme [51], the pose established parallel to the Heme group (Figure 6A) also favored interaction with the cofactor (Hem 901).

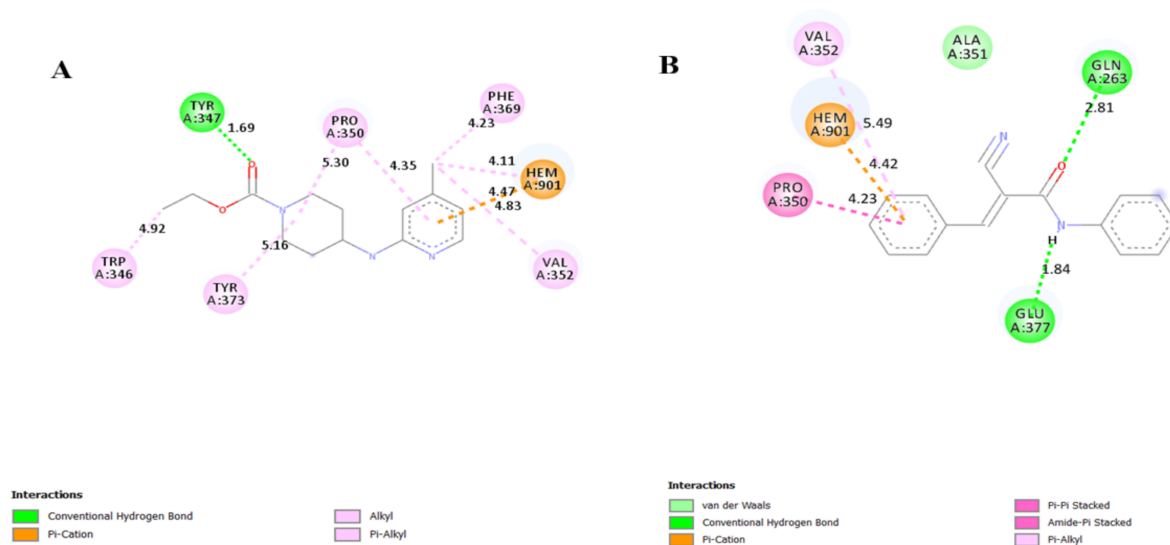


**Figure 7.** Ligand AR-C95791 (A) and JMPR-01 (B) in iNOS target (PDB ID: 3E7G).

Delineation of the affinity of JMPR-01 with PDE4 (an isoform that has specific hydrolyzing capacity on cAMP—a second messenger with modulatory action on effector cells in the pathogenesis of inflammation) was also tested [52]. PDE4 as an inhibited pharmacological target is correlated with a consequent intracellular accumulation of cAMP, which can directly activate protein kinase A (PKA) (responsible for phosphorylation of cAMP-responsive protein (CREB) and activating factor of transcription (ATF-1)), leading to increased synthesis of anti-inflammatory cytokines [53].

Roflumilast is a potent selective PDE4 inhibitor, presenting IC<sub>50</sub> = 0.8 nM against PDE4 expressed in human neutrophils [54]. Figure 8 presents roflumilast and JMPR-01 with the PDE4B target. Certain shared interactions with amino acid residues (Ile 410, Asn 395, Asp 392, and His 234) are highlighted. JMPR-01 interacted in a complementary way with Ser 394 and Pro 396, as well as presented higher quality interactions at the active site, through hydrogen bonds and shorter distance charge transfer interactions, resulting in a higher interactive force and lower free binding energy values as compared to roflumilast.

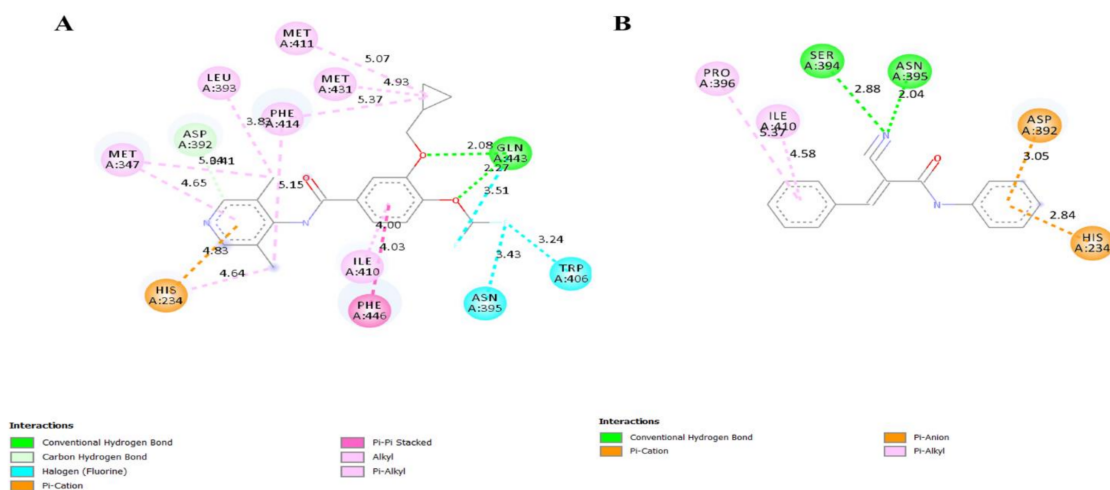


**Figure 8.** Ligand Roflumilast (A) and JMPR-01 (B) in PDE4B target (PDB ID: 1XMU).

The influence of COX-2 in anti-inflammatory therapy is suggested, which highlights its specific up-regulation at the site of inflammation, mainly in response to the local release of cytokines such as IL-1 and TNF- $\alpha$ , activators of the NF- $\kappa$ B transcription factor [55]. Through the metabolism of arachidonic acid, these generate pro-inflammatory and vasoactive eicosanoids such as prostaglandins (PGD2, PGE2, PGF2 $\alpha$ ), prostacyclins (PGI2), and thromboxanes (TXA2) [56]. Thus, its selective inhibition is an effective way to obtain anti-inflammatory, analgesic, and antipyretic activity without harming the physiological actions inherent to COX-1, a target inhibited by traditional NSAIDs [57].

The selective inhibitor Celecoxib, ( $IC_{50} = 0.132 \pm 0.005 \mu\text{M}$  against COX-2), establishes interactions with amino acid residues related to selective inhibition of the enzyme, such as Ser 339, Arg 499, Phe 504 and Val 509, as observed in Figure 9 [58]. JMPR-01, being directed to the more selective region (Val 509), also shares interactions with residues Trp 373, Met 508, and Leu 370, as well as with Ala 502 and Tyr 371. Therefore, JMPR-01 demonstrated inhibition potential that corroborates the results obtained in the *in vivo* assays, where leukocyte migration and edema formation are significantly induced by PGE2, together with the chemotactic and vasoactive action of leukotrienes [56].

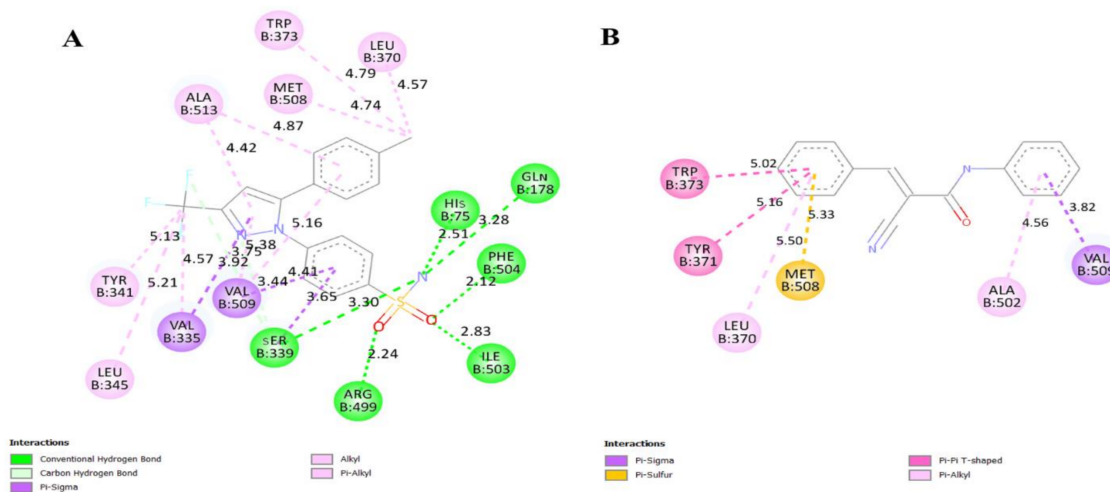


**Figure 9.** Ligand Celecoxib (A) and JMPR-01 (B) in COX-2 target (PDB ID: 3LN1).

Arachidonic acid is also a 5-LOX substrate, and characterized as a crucial point in synthesis of leukotrienes and lipoxins, which are, respectively, (initiation and resolution)

considered regulators of inflammation through association with the 5-LO activating protein (FLAP), the metabolite is 5-hydroperoxyeicosatetraenoic acid (5-HPETE) and, in a subsequent dehydration reaction, the leukotrienes A4 (LTA4). These, in turn, are substrates for the enzyme LTC4 synthase, responsible for the biosynthesis of cystenyl-leukotrienes (CisLT) and for LTA4H in catalysis of the final step in LTB4 biosynthesis, which is a recognized lipid chemotactic mediator and leukocyte activator [59,60].

Further, the action of JMPR-01 in 5-LOX and LTA4 hydrolase enhances its inhibitory effect on the synthesis of leukotrienes and consequent reduction in leukocyte migration, which was indicated in the zymosan induced peritonitis model. According to Sailer et al. (1996) [61], the AKBA ligand co-crystallized to the target 5-LOX presents an  $IC_{50} = 1.5 \mu M$  in relation to the enzyme expressed by peritoneal polymorphonuclear leukocytes. The active AKBA site is allosteric to the catalytic portion, where it binds to residues His 130, Arg 101, and Thr 137 through hydrogen bonds, shown in Figure 10 [62].

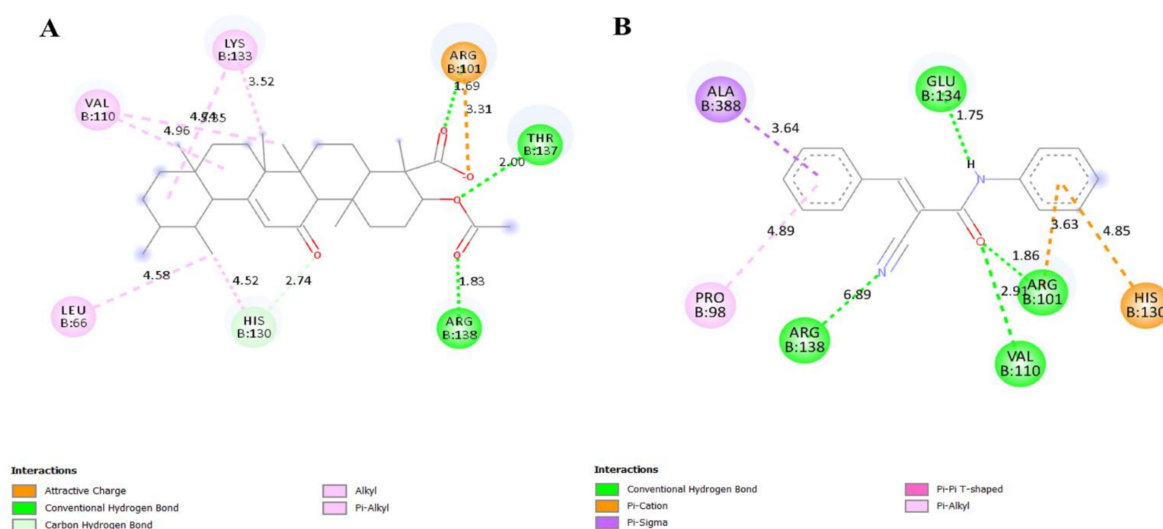


**Figure 10.** Ligand AKBA (A) and JMPR-01 (B) in 5-LOX target (PDB ID: 6NCF).

JMPR-01 interacted with two highlighted residues (His 130 and Arg 101) and also shared interactions with Val 110 and Arg 138. Further, the complementary portion composed of Glu 134, Ala 388, and Pro 98 was indicated. Yet the compound under study presented greater affinity for the enzyme LTA4 hydrolase, with a free binding energy close to the co-crystallized ligand, Bestatin, which is a reversible inhibitor of this enzyme with  $IC_{50} = 4.0 \pm 0.8 \mu M$  [63]. In Figure 11, an interactive overlap suggests influence on the catalytic domain of the target ( $Zn^{2+}$  coordinated by His 295, His 299, and Glu 318) from interactions with His 295, and  $Zn^{2+}$  that are essential for LTB4 biosynthesis of [64].

Through in silico studies, carried out in molecular docking, it was possible to predict the affinity and behavior of JMPR-01 in the catalytic sites of important inflammation targets, with satisfactory results in the enzymes: iNOs, PDE 4B and LTA4H. Inhibition of these targets suggests possible molecular mechanisms for further investigation in more specific in vitro and in vivo assays.



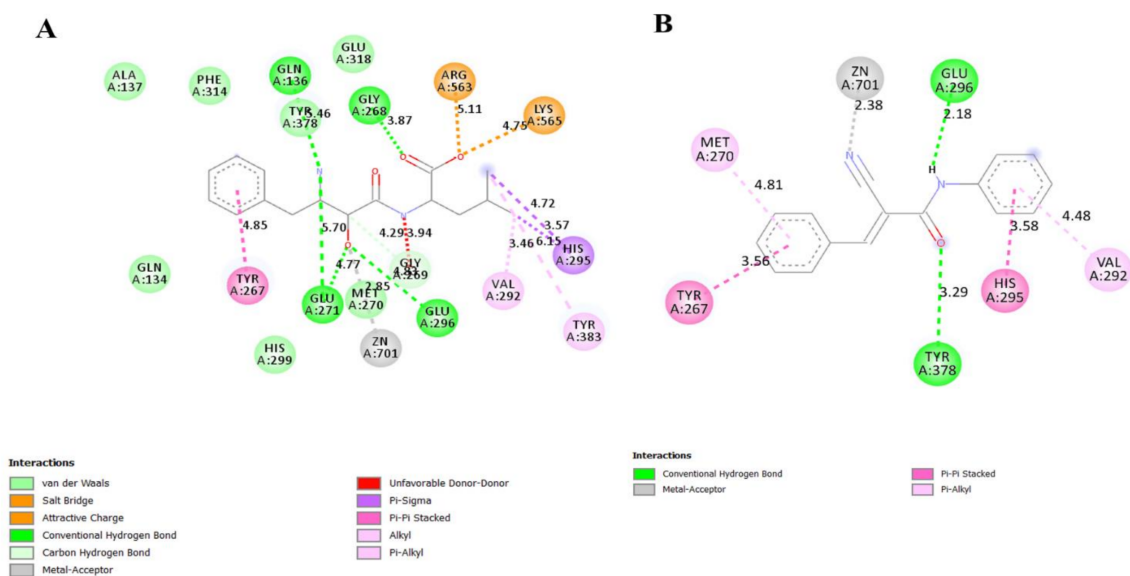


**Figure 11.** Ligand Bestatin (A) and JMPR-01 (B) in LTA4 Hydrolase target (PDB ID: 1HS6).

## 5. Discussion

The compound under study is a synthetic phenylacrylamide: 2-cyano-N-3-diphenylacrylamide derivative (JMPR-01), obtained by the *Knoevenagel* condensation reaction, structurally elucidated by  $^1\text{H}$  and  $^{13}\text{C}$  NMR techniques, in addition to infrared (IR) and mass spectrometry techniques, showing signs that characterized their main substituent groups, namely, the amide group, the benzene ring systems and the cyano group. It is noteworthy that phenylacrylamide derivatives have already been reported in the literature showing a promising result, affirming the molecule as a good drug candidate. Existing studies include the evaluation of the cytotoxic activity of 2-phenylacrylamide derivatives [65] and the evaluation of the anti-inflammatory activity of cyano-phenylacrylamide hybrid derived from indomethacin and paracetamol [8].

The inflammatory process is mediated by multiple agents. Experimental evaluation in inflammation models is necessary for a good understanding at the molecular level of the substance's action. Cytotoxicity assays performed demonstrated that the compound JMPR-1 initiated the induction of cytotoxic effects at a concentration of 100  $\mu\text{M}$ , without significant changes up to a period of 72 h. In addition to the assessment of cytotoxicity and cell viability alteration, the study compound at concentrations of 50–3.125  $\mu\text{M}$  promoted a significant reduction ( $p < 0.05$ ) in nitrite production compared to the unstimulated control group, and also inhibited the TNF- $\alpha$  at all concentrations (50 to 3.125  $\mu\text{M}$ ), thus demonstrating a possible modulation of nitric oxide synthases and reduced expression of TNF- $\alpha$ .

TNF- $\alpha$  is a pleiotropic cytokine, inducing the production of IL-1 and IL-6. Together, these factors promote cellular processes such as chemotaxis, increased vascular permeability and hyperalgesia. IL-1 $\beta$  is directly related to increased excitability and sensitization of nociceptive endings, in addition to inducing apoptosis in the responses of inflammatory and carcinogenic processes [66]. These cytokines, as well as endotoxins, such as lipopolysaccharides (LPS), promote the activation of the endothelium cells through the Toll-like receptor 4 (TLR4) and the RIG-I pathway, which promotes cytokine secretion and the expression of molecules of adhesion, such as E-selectin, VCAM-1 and ICAM-1 to facilitate leukocyte extravasation. Tissue damage arises with increased leukocyte migration due to the secretion of large amounts of inflammatory mediators and reactive molecules, which aggravate the inflammatory process [67].

Cytokines are essential mediators for the development of autoimmune and inflammatory pathologies, a result of the induction of the TNF- $\alpha$  signal, including the activation of NF- $\kappa\text{B}$ , ERK, p38 MAPK and JNK, which are gene activation pathways for IL-1 $\beta$ , IL-8, IL-6, chemokines, adhesion molecules and immunological enzymes, such as iNOs itself [68,69].

TNF- $\alpha$ , as well as IL-1, influence the activity of the signaling pathway for the NF- $\kappa$ B transcription factor, which regulates the gene expression of inflammatory mediators (these cytokines are overexpressed when this signaling pathway is activated by stress oxidative). This family of cytokines is composed of structurally related members, including NF- $\kappa$ B1 (p50/p105), NF- $\kappa$ B2 (p52/p100), RelA (p65), RelB and c-Rel that are normally inactivated in the cytoplasm by inhibitory I $\kappa$ B proteins, mainly I $\kappa$ B $\alpha$  [70,71].

These cytokines, in turn, act on both canonical and non-canonical NF- $\kappa$ B activation pathways, activating the I $\kappa$ B kinase complex (IKK), which then mediates phosphorylation, ubiquitination and degradation of I $\kappa$ B and free NF- $\kappa$ B dimer translocation to the nucleus to initiate gene transcription (canonical pathway). The non-canonical pathway involves phosphorylation of the inhibitory domains of p100 and p105 and also results in the release of the NF- $\kappa$ B dimer. Activation of this signaling pathway is important, as it results in the expression of several inflammatory mediators, including many enzymes, such as inducible nitric oxide synthase (iNOS), cyclooxygenases and lipoxygenases that exert pro-inflammatory effects [72,73].

The action of the compound JMPR-1 as a modulator of nitric oxide (NO) synthases was also visualized through Molecular Docking simulations, since the score obtained by the test compound was more negative than that obtained by the co-crystallized ligand; besides that, it also established important interactions with the amino acid residues Glu 263 and Glu 377 that are essential for the inhibitory activity of this target.

The regulation of the activity of iNOS isoforms is important to maintain the physiological responses and control the deleterious effects mediated by NO [49]; thus, inhibition is part of the clinical management in many inflammatory diseases. Therefore, the inhibition of iNOS, as a result of the suppression of cytokines, chemokines and adhesion molecules, in addition to the maintenance of vascular tone and permeability, (as suggested in the present paw edema model in this study, and also the affinity of the compound tested for iNOS) is related to the observed in vitro modulation of nitrite production [37,74].

Based on the observed reduced expression of TNF- $\alpha$ , IL-1 $\beta$ , and nitrite in vitro, it can be inferred that a regulatory mechanism is correlated with this transcriptional pathway effect, including a possible decrease in oxidative stress, and inhibition of key regulators of the NF- $\kappa$ B pathway. There are few studies evaluating the performance of phenylacrylamide derivatives in this effect, but they do suggest that their Michael acceptor regions bind to cysteine residues in Keap-1 cytosolic proteins, which act as redox sensors and negative regulators of Nrf2 (nuclear factor erythroid 2 related factor 2), activating the expression of antioxidant and anti-inflammatory enzymes [23–25].

In evaluating the anti-inflammatory activity in in vivo models, JMPR-01 significantly inhibited ( $p < 0.05$ ) the migration of leukocytes by 61.8, 68.5 and 90.5%, at the respective doses of 5, 10 and 50 mg/kg, assuming a better performance when compared to the control, which corresponded to indomethacin. Similarly, in the in situ inflammation model, the paw edema that JMPR-01 at a dose of 50 mg/kg inhibited the formation of edema from 6 h onwards, with cessation of activity within 24 h, could be visualized. Using the compound at a higher dose (100 mg/kg), satisfactory inhibition was observed from 2 to 6 h, with activity similar to that of Dexamethasone control, but not significantly maintained after 24 h.

Inflammatory mediators directly involved in the recruitment of leukocytes have been widely studied with the aim of elucidating their mechanisms of action. Despite a well elucidated chemotactic activity [75], Tager et al. [76] identified the involvement of Leukotriene B4 (LTB4) in the recruitment of CD-4 + T lymphocytes through the BLT-1 receptor and demonstrated that LTB4/BLT-1 T cell-mediated chemotactic activity compared to CXCL12 is one of the most effective T cell chemoattractants. An in vitro complementary study also revealed that CD-8+ T cells, after stimulation by IL-2, acquired chemotactic sensitivity to LTB4 (when released by previously activated mast cells) [77].

Cytokines such as TNF- $\alpha$ , IL-1, and IL-4 also play important roles in chemotaxis, acting through the up-regulation of vascular adhesion molecules, specifically E-selectin, P-selectin,

and the cell adhesion molecule (ICAM -1), promoting fixation and rolling of leukocytes inside the vessel [78]. These data corroborate *in vitro* human umbilical vein endothelial cell studies, where it was observed that IL1- $\beta$  and TNF- $\alpha$  mediate eosinophil adhesion and trans endothelial migration, thereby stimulating the release of ICAM-1 (intercellular adhesion molecule-1) E-selectin, and VCAM-1 (vascular cell adhesion molecule-1) [34].

The reduction in cytokine production disfavors COX-2 transcription through the NF $\kappa$ B pathway. In the edematogenic activity, COX-2 transcription stands out for the biosynthesis of eicosanoids, including prostaglandin E1 (PGE1), prostaglandin E2 (PGE2) and prostacyclin I2 [56]. Together, they participate in the vascular phase of inflammation, promoting vasodilation and increased permeability of the venule with consequent plasma exudation [36,56]. These, in particular PGE1 and PGE2, are capable of sensitizing afferent nociceptive nerve terminals to endogenous pain mediators, such as bradykinin, histamine and serotonin, which are intrinsically related to hyperalgesia [79].

Dexamethasone was chosen as the standard for *in vitro* tests of nitrite and cytokine dosages, as well as in paw edema, due to its good performance in anti-inflammatory and immunomodulatory therapy. Its mechanism involves the action on nuclear receptors involved in the transcription of anti-inflammatory mediators [80], among which we highlight those of protein origin, such as Annexin A1, known as a potent multifunctional anti-inflammatory mediator. It is known that the activity of Annexin A1 comes mainly from its active grouping called N-terminal peptide Ac2-26, which binds to the formyl-peptide receptor (FPR) grouping, promoting reduction in the production of the storm of pro-inflammatory cytokines [81]. The direct correlation between glucocorticoids and Annexin A1 can be described in *in vivo* studies using mice deficient in Annexin A1, where it was possible to observe an absence of response to administered glucocorticoids [82,83].

Studies by Pupjalis et al., 2011 [84], using apoptotic immune cells, demonstrated that dexamethasone-mediated Annexin A1 expression contributed to TNF- $\alpha$  suppression by a mechanism involving formyl peptide receptors (FPR). These data corroborate *in vitro* studies by Gobetti and Cooray, 2016 [85], involving fibroblasts present in chronic inflammatory lung diseases, where it was possible to identify that mimicking the actions of Annexin A1 may have positive therapeutic effects in these pathologies, through the regulation of the NF $\kappa$ -B pathway was induced by TNF- $\alpha$ , a mediator that had its release suppressed by JMPR-01 in *in vitro* studies. The suppressive activity of TNF- $\alpha$  presented by JMPR-01 opens doors for further investigations addressing the possible role of the same in increasing the expression of Annexin A1 or in promoting activities similar to the protein itself.

This action in the reduction of mediators can be justified by Molecular Docking, in which the compound JMPR-1 established important interactions, proving a possible action in the pathways of COX-2, 5-Lox and leukotrienes, which can be useful for conducting studies futures, as well as proof of activities that cannot be experimentally validated. Our results suggest possible mechanisms of action of phenylacrylamide derivatives towards the inhibition of inflammatory mediators involved in inflammatory signaling, and allow for future development of promising drugs to treat inflammatory diseases.

## 6. Conclusions

In conclusion, this study presents for the first time the anti-inflammatory potential of a new phenylacrylamide derivative obtained through bioisosteric ring modification of a previously studied drug. Using *in vitro* and *in vivo* approaches, immunomodulatory and anti-inflammatory properties were demonstrated, suggesting that its mechanism (in part) may be related to decreased expression of inflammatory cytokines (TNF- $\alpha$  and IL-1 $\beta$ ) and nitric oxide. In the *in silico* studies, satisfactory couplings were observed for targets such as iNOs, COX-2 and PDE-IV, suggesting potentially multi-target interactions involving the inflammatory response. This can be further investigated. These preliminary results demonstrate the therapeutic potential of JMPR-01, making it a potential drug for inflammatory conditions, with both viable synthesis and low production costs.

**Supplementary Materials:** The following supporting information can be downloaded at: <https://www.mdpi.com/article/10.3390/pharmaceutics14010188/s1>, Figure S1: FT-IR spectrum of JMPR-01; Figure S2: <sup>1</sup>H NMR spectrum of JMPR-01 (500 MHz, DMSO-d<sub>6</sub>); Figure S3: <sup>13</sup>C NMR spectrum of JMPR-01 (125 MHz, DMSO-d<sub>6</sub>); Figure S4 HRMS m/z [M+H] of JMPR-01 (MALDI-TOF); Figure S5 Differential Scanning Calorimetry (DSC) (A) and Thermogravimetric Analysis (B) of JMPR-01; Table S1: CC50, EC50 and Selectivity Index of JMPR-01 standardized by TNF- $\alpha$  inhibition in determined in cultures of J774 macrophages.

**Author Contributions:** Participated in research design: P.R.d.S., V.L.d.S., R.O.d.M. and C.F.V.; performed the experiments and the data analysis: P.R.d.S., R.F.d.E.S., C.d.O.M., F.E.P.C., T.B.C., Y.V.B., Y.M.S.d.M.e.S. and N.F.d.S.; wrote or contributed to the writing of the manuscript: P.R.d.S., V.L.d.S., R.O.d.M., C.F.V., F.E.P.C., T.B.C., Y.V.B. and Y.M.S.d.M.e.S. All authors have read and agreed to the published version of the manuscript.

**Funding:** This research received no external funding.

**Institutional Review Board Statement:** Animal use protocol 003/2021 was approved by the Ethics Committee on Animal from the State University of Paraíba and all procedures were performed in accordance with the NIH Guidelines for the Care and Use of Laboratory Animal.

**Informed Consent Statement:** Not applicable.

**Data Availability Statement:** Data can be requested by contacting the corresponding author.

**Acknowledgments:** This study was financed in part by the State University of Paraíba grant 001/2021, Fundação de Amparo à Pesquisa do Estado da Paraíba (FAPESQ), Coordenação de Aperfeiçoamento de Pessoal de Nível Superior (Capes) with collaboration from the Universidade Federal da Bahia (UFBA).

**Conflicts of Interest:** The authors declare no conflict of interest. The founding sponsors had no role in the design of the study; in the collection, analyses, or interpretation of data; in the writing of the manuscript, and in the decision to publish the results.

## References

1. Mortaz, E.; Pourdolat, G.; Varahram, M.; Tabarsi, P.; Farnia, P.; Garssen, J.; Adcock, I. Investigation of CD14 with toll like receptors expression in pleural effusion for detection of thoracic disorders. *Eur. Respir. Soc.* **2017**, *50*, PA1588.
2. Chen, L.; Deng, H.; Cui, H.; Fang, J.; Zuo, Z.; Deng, J.; Li, Y.; Wang, X.; Zhao, L. Inflammatory responses and inflammation-associated diseases in organs. *Oncotarget* **2018**, *9*, 7204–7218. [[CrossRef](#)] [[PubMed](#)]
3. Grosser, T.; Smyth, E.; Fitzgerald, G. *Anti-Inflammatory, Antipyretic, and Analgesic Agents; Pharmacotherapy of Gout*; ResearchGate: Berlin, Germany, 2011.
4. Murakami, M.; Hirano, T. The molecular mechanisms of chronic inflammation development. *Front. Immunol.* **2012**, *3*, 1–2. [[CrossRef](#)]
5. Marmitt, D.J.; Rempel, C.; Goettert, M.I.; Silva, A.C. Plantas Mediciniais da RENISUS Com Potencial Anti-inflamatório: Revisão Sistemática Em Três Bases de Dados Científicas. *Rev. Fitos* **2015**, *9*, 129–144. [[CrossRef](#)]
6. Bordoni, A.; Danesi, F.; Dardevet, D.; Dupont, D.; Fernandez, A.S.; Gille, D.; Nunes dos Santos, C.; Pinto, P.; Re, R.; Rémond, D.; et al. Dairy products and inflammation: A review of the clinical evidence. *Crit. Rev. Food Sci. Nutr.* **2017**, *57*, 2497–2525. [[CrossRef](#)]
7. Gene, E.; Calvet, X.; Moron, A.; Iglesias, M. Recommendations for the use of anti-inflammatory drugs and indications for gastrointestinal protection in emergency departments. *Emergencias* **2009**, *21*, 295–300.
8. Silva, P.; de Almeida, M.; Silva, J.; Albino, S.; Espírito-Santo, R.; Lima, M.; Villarreal, C.; Moura, R.; Santos, V. (E)-2-Cyano-3-(1H-Indol-3-yl)-N-phenylacrylamide, a hybrid compound derived from indomethacin and paracetamol: Design, synthesis and evaluation of the anti-inflammatory potential. *Int. J. Mol. Sci.* **2020**, *21*, 2591. [[CrossRef](#)] [[PubMed](#)]
9. Eilenberger, C.; Kratz, S.R.A.; Rothbauer, M.; Ehmoser, E.K.; Ertl, P.; Küpcü, S. Optimized alamarBlue assay protocol for drug dose-response determination of 3D tumor spheroids. *MethodsX* **2018**, *5*, 781–787. [[CrossRef](#)]
10. Espírito-Santo, R.F.; Meira, C.S.; Dos Santos Costa, R.; Filho, O.P.S.; Evangelista, A.F.; Trossini, G.H.G.; Ferreira, G.M.; Da Silva Velozo, E.; Villarreal, C.F.; Pereira Soares, M.B. The anti-inflammatory and immunomodulatory potential of braylin: Pharmacological properties and mechanisms by in silico, in vitro and in vivo approaches. *PLoS ONE* **2017**, *12*, e0179174. [[CrossRef](#)] [[PubMed](#)]
11. Green, L.C.; Wagner, D.A.; Glogowski, J.; Skipper, P.L.; Wishnok, J.S.; Tannenbaum, S.R. Analysis of nitrate, nitrite, and [15N] nitrate in biological fluids. *Anal. Biochem.* **1982**, *126*, 131–138. [[CrossRef](#)]



12. de Moraes Oliveira-Tintino, C.D.; Pessoa, R.T.; Fernandes, M.N.M.; Alcântara, I.S.; da Silva, B.A.F.; de Oliveira, M.R.C.; Martins, A.O.B.P.B.; da Silva, M.d.S.; Tintino, S.R.; Rodrigues, F.F.G.; et al. Anti-inflammatory and anti-edematogenic action of the *Croton campestris* A. St.-Hil (Euphorbiaceae) essential oil and the compound  $\beta$ -caryophyllene in in vivo models. *Phytomedicine* **2018**, *41*, 82–95. [[CrossRef](#)]
13. Vinegar, R.; Truax, J.F.; Selph, J.L. Some Quantitative Temporal Characteristics of Carrageenin-Induced Pleurisy in the Rat. *Proc. Soc. Exp. Biol. Med.* **1973**, *143*, 711–714. [[CrossRef](#)] [[PubMed](#)]
14. da Lima, M.S.; Quintans-Júnior, L.J.; de Santana, W.A.; Martins Kaneto, C.; Pereira Soares, M.B.; Villarreal, C.F. Anti-inflammatory effects of carvacrol: Evidence for a key role of interleukin-10. *Eur. J. Pharmacol.* **2013**, *699*, 112–117. [[CrossRef](#)] [[PubMed](#)]
15. Moraes, A.D.T.d.O.; de Miranda, M.D.S.; Jacob, Í.T.T.; Amorim, C.A.d.C.; de Moura, R.O.; da Silva, S.Â.S.; Soares, M.B.P.; de Almeida, S.M.V.; Souza, T.R.C.d.L.; de Oliveira, J.F.; et al. Synthesis, in vitro and in vivo biological evaluation, COX-1/2 inhibition and molecular docking study of indole-N-acylhydrazone derivatives. *Bioorg. Med. Chem.* **2018**, *26*, 5388–5396. [[CrossRef](#)] [[PubMed](#)]
16. Chandak, N.; Kumar, P.; Kaushik, P.; Varshney, P.; Sharma, C.; Kaushik, D.; Jain, S.; Aneja, K.R.; Sharma, P.K. Dual evaluation of some novel 2-amino-substituted coumarinylthiazoles as anti-inflammatory-antimicrobial agents and their docking studies with COX-1/COX-2 active sites. *J. Enzym. Inhib. Med. Chem.* **2014**, *29*, 476–484. [[CrossRef](#)]
17. Appaturi, J.N.; Selvaraj, M.; Abdul Hamid, S.B.; Bin Johan, M.R. Synthesis of 3-(2-furylmethylene)-2,4-pentanedione using DL-Alanine functionalized MCM-41 catalyst via *Knoevenagel* condensation reaction. *Microporous Mesoporous Mater.* **2018**, *260*, 260–269. [[CrossRef](#)]
18. Wach, A.; Drozdek, M.; Dudek, B.; Szneler, E.; Kuśtrowski, P. Control of amine functionality distribution in polyvinylamine/SBA-15 hybrid catalysts for *Knoevenagel* condensation. *Catal. Commun.* **2015**, *64*, 52–57. [[CrossRef](#)]
19. Li, J.P.H.; Adesina, A.A.; Kennedy, E.M.; Stockenhuber, M. A mechanistic study of the *Knoevenagel* condensation reaction: New insights into the influence of acid and base properties of mixed metal oxide catalysts on the catalytic activity. *Phys. Chem. Chem. Phys.* **2017**, *19*, 26630–26644. [[CrossRef](#)] [[PubMed](#)]
20. Rampersad, S.N. Multiple applications of alamar blue as an indicator of metabolic function and cellular health in cell viability bioassays. *Sensors* **2012**, *12*, 12347–12360. [[CrossRef](#)] [[PubMed](#)]
21. Feng, L.; Sun, Y.; Song, P.; Xu, L.; Wu, X.; Wu, X.; Shen, Y.; Sun, Y.; Kong, L.; Wu, X.; et al. Seselin ameliorates inflammation via targeting Jak2 to suppress the proinflammatory phenotype of macrophages. *Br. J. Pharmacol.* **2019**, *176*, 317–333. [[CrossRef](#)] [[PubMed](#)]
22. Lambden, S. Bench to bedside review: Therapeutic modulation of nitric oxide in sepsis—An update. *Intensive Care Med. Exp.* **2019**, *7*, 64. [[CrossRef](#)]
23. Rahat, M.A.; Hemmerlein, B. Macrophage-tumor cell interactions regulate the function of nitric oxide. *Front. Physiol.* **2013**, *4*, 144. [[CrossRef](#)]
24. De Moraes Pultrini, A.; Almeida Galindo, L.; Costa, M. Effects of the essential oil from *Citrus aurantium* L. in experimental anxiety models in mice. *Life Sci.* **2006**, *78*, 1720–1725. [[CrossRef](#)]
25. De Freitas Silva, M.; Pruccoli, L.; Morrioni, F.; Sita, G.; Seghetti, F.; Viegas, C.; Tarozzi, A. The Keap1/Nrf2-ARE pathway as a pharmacological target for chalcones. *Molecules* **2018**, *23*, 1803. [[CrossRef](#)]
26. Gu, X.; Chen, J.; Zhang, Y.; Guan, M.; Li, X.; Zhou, Q.; Song, Q.; Qiu, J. Synthesis and assessment of phenylacrylamide derivatives as potential anti-oxidant and anti-inflammatory agents. *Eur. J. Med. Chem.* **2019**, *180*, 62–71. [[CrossRef](#)]
27. Rudziak, P.; Ellis, C.G.; Kowalewska, P.M. Role and molecular mechanisms of pericytes in regulation of leukocyte diapedesis in inflamed tissues. *Mediat. Inflamm.* **2019**, *2019*, 4123605. [[CrossRef](#)]
28. Nourshargh, S.; Alon, R. Leukocyte Migration into Inflamed Tissues. *Immunity* **2014**, *41*, 694–707. [[CrossRef](#)] [[PubMed](#)]
29. Cash, J.L.; White, G.E.; Greaves, D.R. *Chapter 17 Zymosan-Induced Peritonitis as a Simple Experimental System for the Study of Inflammation*, 1st ed.; Elsevier Inc.: Amsterdam, The Netherlands, 2009; Volume 461, ISBN 9780123749079.
30. Volman, T.J.H.; Hendriks, T.; Goris, R.J.A. Zymosan-induced generalized inflammation: Experimental studies into mechanisms leading to multiple organ dysfunction syndrome. *Shock* **2005**, *23*, 291–297. [[CrossRef](#)] [[PubMed](#)]
31. Underhill, D.M. Macrophage recognition of zymosan particles. *J. Endotoxin Res.* **2003**, *9*, 176–180. [[CrossRef](#)] [[PubMed](#)]
32. Deng, X.; Wang, X.; Andersson, R. Alterations in endothelial barrier permeability in multiple organs during overactivation of macrophages in rats 1996. *Shock* **1996**, *6*, 126–133. [[CrossRef](#)]
33. Ley, K. Molecular mechanisms of leukocyte recruitment in the inflammatory process. *Cardiovasc. Res.* **1996**, *32*, 733–742. [[CrossRef](#)]
34. Wong, C.H.Y.; Heit, B.; Kubes, P. Molecular regulators of leucocyte chemotaxis during inflammation. *Cardiovasc. Res.* **2010**, *86*, 183–191. [[CrossRef](#)] [[PubMed](#)]
35. Ebisawa, M.; Bochner, B.S.; Georas, S.N.; Schleimer, R.P. Eosinophil transendothelial migration induced by cytokines. I. Role of endothelial and eosinophil adhesion molecules in IL-1 beta-induced transendothelial migration. *J. Immunol.* **1992**, *149*, 4021–4028.
36. Alessandri, A.L.; Sousa, L.P.; Lucas, C.D.; Rossi, A.G.; Pinho, V.; Teixeira, M.M. Resolution of inflammation: Mechanisms and opportunity for drug development. *Pharmacol. Ther.* **2013**, *139*, 189–212. [[CrossRef](#)] [[PubMed](#)]
37. Saldanha, A.A.; Vieira, L.; Ribeiro, R.I.M.d.A.; Thomé, R.G.; dos Santos, H.B.; Silva, D.B.; Carollo, C.A.; de Oliveira, F.M.; de Oliveira Lopes, D.; de Siqueira, J.M.; et al. Chemical composition and evaluation of the anti-inflammatory and antinociceptive activities of *Duguetia furfuracea* essential oil: Effect on edema, leukocyte recruitment, tumor necrosis factor alpha production, iNOS expression, and adenosinergic and opioid. *J. Ethnopharmacol.* **2019**, *231*, 325–336. [[CrossRef](#)] [[PubMed](#)]

38. Zhao, X.H.; Zhang, T.; Li, Y.Q. The up-regulation of spinal Toll-like receptor 4 in rats with inflammatory pain induced by complete Freund's adjuvant. *Brain Res. Bull.* **2015**, *111*, 97–103. [[CrossRef](#)]
39. Nisar, A.; Akhter, N.; Singh, G.; Masood, A.; Malik, A.; Banday, B.; Zargar, M.A. Modulation of T-helper cytokines and inflammatory mediators by *Atropa accuminata*. Royle in adjuvant induced arthritic tissues. *J. Ethnopharmacol.* **2015**, *162*, 215–224. [[CrossRef](#)]
40. Ben, I.O.; Woode, E.; Koffuor, G.A.; Boakye-Gyasi, E.; Titiloye, N.A. Effect of *trichilia monadelpha* (Meliaceae) extracts on bone histomorphology in complete Freund's adjuvant-induced arthritis. *J. Intercult. Ethnopharmacol.* **2017**, *6*, 177–185. [[CrossRef](#)]
41. Gris, G.; Merlos, M.; Vela, J.M.; Zamanillo, D.; Portillo-Salido, E. S1RA, a selective sigma-1 receptor antagonist, inhibits inflammatory pain in the carrageenan and complete Freund's adjuvant models in mice. *Behav. Pharmacol.* **2014**, *25*, 226–235. [[CrossRef](#)] [[PubMed](#)]
42. Xiang, H.C.; Lin, L.X.; Hu, X.F.; Zhu, H.; Li, H.P.; Zhang, R.Y.; Hu, L.; Liu, W.T.; Zhao, Y.L.; Shu, Y.; et al. AMPK activation attenuates inflammatory pain through inhibiting NF- $\kappa$ B activation and IL-1 $\beta$  expression. *J. Neuroinflamm.* **2019**, *16*, 34. [[CrossRef](#)]
43. Cui, L.; Feng, L.; Zhang, Z.H.; Jia, X. Bin The anti-inflammation effect of baicalin on experimental colitis through inhibiting TLR4/NF- $\kappa$ B pathway activation. *Int. Immunopharmacol.* **2014**, *23*, 294–303. [[CrossRef](#)] [[PubMed](#)]
44. Ghasemi, M. *Nitric Oxide: Antidepressant Mechanisms and Inflammation*, 1st ed.; Elsevier Inc.: Amsterdam, The Netherlands, 2019; Volume 86, ISBN 9780128166680.
45. Meng, X.-Y.; Zhang, H.-X.; Mezei, M.; Cui, M. Molecular Docking: A Powerful Approach for Structure-Based Drug Discovery. *Curr. Comput. Aided-Drug Des.* **2012**, *7*, 146–157. [[CrossRef](#)]
46. Pinzi, L.; Rastelli, G. Molecular docking: Shifting paradigms in drug discovery. *Int. J. Mol. Sci.* **2019**, *20*, 4331. [[CrossRef](#)]
47. Gupta, M.; Sharma, R.; Kumar, A. Docking techniques in pharmacology: How much promising? *Comput. Biol. Chem.* **2018**, *76*, 210–217. [[CrossRef](#)] [[PubMed](#)]
48. Westermaier, Y.; Barril, X.; Scapozza, L. Virtual screening: An in silico tool for interlacing the chemical universe with the proteome. *Methods* **2015**, *71*, 44–57. [[CrossRef](#)]
49. Singh, M.; Padhy, G.; Vats, P.; Bhargava, K.; Sethy, N.K. Hypobaric hypoxia induced arginase expression limits nitric oxide availability and signaling in rodent heart. *Biochim. Biophys. Acta -Gen. Subj.* **2014**, *1840*, 1817–1824. [[CrossRef](#)]
50. Lee, W.; Yang, S.; Lee, C.; Park, E.K.; Kim, K.M.; Ku, S.K.; Bae, J.S. Aloin reduces inflammatory gene iNOS via inhibition activity and p-STAT-1 and NF- $\kappa$ B. *Food Chem. Toxicol.* **2019**, *126*, 67–71. [[CrossRef](#)]
51. Garcin, E.D.; Arvai, A.S.; Rosenfeld, R.J.; Kroeger, M.D.; Crane, B.R.; Andersson, G.; Andrews, G.; Hamley, P.J.; Mallinder, P.R.; Nicholls, D.J.; et al. Anchored plasticity opens doors for selective inhibitor design in nitric oxide synthase. *Nat. Chem. Biol.* **2008**, *4*, 700–707. [[CrossRef](#)] [[PubMed](#)]
52. Chiricozzi, A.; Caposiena, D.; Garofalo, V.; Cannizzaro, M.V.; Chimenti, S.; Saraceno, R. A new therapeutic for the treatment of moderate-to-severe plaque psoriasis: Apremilast. *Expert Rev. Clin. Immunol.* **2016**, *12*, 237–249. [[CrossRef](#)]
53. Li, H.; Zuo, J.; Tang, W. Phosphodiesterase-4 inhibitors for the treatment of inflammatory diseases. *Front. Pharmacol.* **2018**, *9*, 1048. [[CrossRef](#)] [[PubMed](#)]
54. Hatzelmann, A.; Schudt, C. Anti-inflammatory and immunomodulatory potential of the novel PDE4 inhibitor roflumilast in vitro. *J. Pharmacol. Exp. Ther.* **2001**, *297*, 267–279.
55. Mendes, R.T.; Stanczyk, C.P.; Sordi, R.; Otuki, M.F.; dos Santos, F.A.; Fernandes, D. Inibição seletiva da ciclo-oxigenase-2: Riscos e benefícios. *Rev. Bras. Reumatol.* **2012**, *52*, 774–782. [[CrossRef](#)]
56. Moreira, V.; Gutiérrez, J.M.; Lomonte, B.; Vinolo, M.A.R.; Curi, R.; Lambeau, G.; Teixeira, C. 12-HETE is a regulator of PGE2 production via COX-2 expression induced by a snake venom group IIA phospholipase A2 in isolated peritoneal macrophages. *Chem. Biol. Interact.* **2020**, *317*, 108903. [[CrossRef](#)] [[PubMed](#)]
57. Meshram, M.A.; Bhise, U.O.; Makhal, P.N.; Kaki, V.R. Synthetically-tailored and nature-derived dual COX-2/5-LOX inhibitors: Structural aspects and SAR. *Eur. J. Med. Chem.* **2021**, *225*, 113804. [[CrossRef](#)] [[PubMed](#)]
58. Sağlık, B.N.; Osmaniye, D.; Levent, S.; Çevik, U.A.; Çavuşoğlu, B.K.; Özkay, Y.; Kaplancıklı, Z.A. Design, synthesis and biological assessment of new selective COX-2 inhibitors including methyl sulfonyl moiety. *Eur. J. Med. Chem.* **2021**, *209*, 112918. [[CrossRef](#)]
59. Wang, X.; Bey, A.L.; Katz, B.M.; Badea, A.; Kim, N.; David, L.K.; Duffney, L.J.; Kumar, S.; Mague, S.D.; Hulbert, S.W.; et al. Altered mGluR5-Homer scaffolds and corticostriatal connectivity in a Shank3 complete knockout model of autism. *Nat. Commun.* **2016**, *7*, 11459. [[CrossRef](#)]
60. Saeki, K.; Yokomizo, T. Identification, signaling, and functions of LTB4 receptors. *Semin. Immunol.* **2017**, *33*, 30–36. [[CrossRef](#)]
61. Sailer, E.R.; Subramanian, L.R.; Rall, B.; Hoernlein, R.F.; Ammon, H.P.T.; Safayhi, H. Acetyl-11-keto- $\beta$ -boswellic acid (AKBA): Structure requirements for binding and 5-lipoxygenase inhibitory activity. *Br. J. Pharmacol.* **1996**, *117*, 615–618. [[CrossRef](#)] [[PubMed](#)]
62. Gilbert, N.C.; Gerstmeier, J.; Schexnaydre, E.E.; Börner, F.; Garscha, U.; Neau, D.B.; Werz, O.; Newcomer, M.E. Structural and mechanistic insights into 5-lipoxygenase inhibition by natural products. *Nat. Chem. Biol.* **2020**, *16*, 783–790. [[CrossRef](#)]
63. Orning, L.; Krivi, G.; Fitzpatrick, F.A. Leukotriene A4 hydrolase. Inhibition by bestatin and intrinsic aminopeptidase activity establish its functional resemblance to metallohydrolase enzymes. *J. Biol. Chem.* **1991**, *266*, 1375–1378. [[CrossRef](#)]
64. Thunnissen, M.M.G.M.; Nordlund, P.; Haeggström, J.Z. Crystal structure of human leukotriene A4 hydrolase, a bifunctional enzyme in inflammation. *Nat. Struct. Biol.* **2001**, *8*, 131–135. [[CrossRef](#)] [[PubMed](#)]

65. Tarleton, M.; Dyson, L.; Gilbert, J.; Sakoff, J.A.; McCluskey, A. Focused library development of 2-phenylacrylamides as broad spectrum cytotoxic agents. *Bioorg. Med. Chem.* **2013**, *21*, 333–347. [[CrossRef](#)] [[PubMed](#)]
66. Dias Quintão, J.L.; Reis Gonzaga, A.C.; Galdino, G.; Lima Romero, T.R.; Silva, J.F.; Lemos, V.S.; Campolina-Silva, G.H.; Aparecida de Oliveira, C.; Bohórquez Mahecha, G.A.; Gama Duarte, I.D. TNF- $\alpha$ , CXCL-1 and IL-1  $\beta$  as activators of the opioid system involved in peripheral analgesic control in mice. *Eur. J. Pharmacol.* **2021**, *896*, 173900. [[CrossRef](#)]
67. Le, K.T.T.; Chu, X.; Jaeger, M.; Plantinga, J.A.; Matzaraki, V.; Withoff, S.; Joosten, L.A.B.; Netea, M.G.; Wijmenga, C.; Li, Y.; et al. Leukocyte-released mediators in response to both bacterial and fungal infections trigger ifn pathways, independent of il-1 and tnf- $\alpha$ , in endothelial cells. *Front. Immunol.* **2019**, *10*, 1–13. [[CrossRef](#)]
68. Pandey, S.; Kawai, T.; Akira, S. Microbial sensing by toll-like receptors and intracellular nucleic acid sensors. *Cold Spring Harb. Perspect. Biol.* **2015**, *7*, 1–18. [[CrossRef](#)] [[PubMed](#)]
69. Brenner, D.; Blaser, H.; Mak, T.W. Regulation of tumour necrosis factor signalling: Live or let die. *Nat. Rev. Immunol.* **2015**, *15*, 362–374. [[CrossRef](#)]
70. Shamroukh, A.H.; Hegab, M.I. A review on synthesis, therapeutic, and computational studies of substituted 1, 3, 4 thiadiazole derivatives. *Egypt. J. Chem.* **2020**, *63*, 4387–4408.
71. Albensi, B.C. What is nuclear factor kappa B (NF- $\kappa$ B) doing in and to the mitochondrion? *Front. Cell Dev. Biol.* **2019**, *7*, 1–7. [[CrossRef](#)] [[PubMed](#)]
72. Rex, J.; Lutz, A.; Faletti, L.E.; Albrecht, U.; Thomas, M.; Bode, J.G.; Borner, C.; Sawodny, O.; Merfort, I. IL-1 $\beta$  and TNF $\alpha$  differentially influence NF- $\kappa$ B activity and FasL-induced apoptosis in primary murine hepatocytes during LPS-induced inflammation. *Front. Physiol.* **2019**, *10*, 1–15. [[CrossRef](#)] [[PubMed](#)]
73. Mussbacher, M.; Salzmann, M.; Brostjan, C.; Hoesel, B.; Schoergenhofer, C.; Datler, H.; Hohensinner, P.; Basílio, J.; Petzelbauer, P.; Assinger, A. Cell type-specific roles of NF- $\kappa$ B linking inflammation and thrombosis. *Front. Immunol.* **2019**, *10*, 85. [[CrossRef](#)]
74. Lee, C.-L.; Chiang, L.-C.; Cheng, L.-H.; Liaw, C.-C.; Abd El-Razek, M.H.; Chang, F.-R.; Wu, Y.-C. Influenza A (H1N1) antiviral and cytotoxic agents from *Ferula assa-foetida*. *J. Nat. Prod.* **2009**, *72*, 1568–1572. [[CrossRef](#)]
75. Yokomizo, T.; Izumi, T.; Shimizu, T. Leukotriene B<sub>4</sub>: Metabolism and signal transduction. *Arch. Biochem. Biophys.* **2001**, *385*, 231–241. [[CrossRef](#)]
76. Tager, A.M.; Bromley, S.K.; Medoff, B.D.; Islam, S.A.; Bercury, S.D.; Friedrich, E.B.; Carafone, A.D.; Gerszten, R.E.; Luster, A.D. Leukotriene B<sub>4</sub> receptor BLT1 mediates early effector T cell recruitment. *Nat. Immunol.* **2003**, *4*, 982–990. [[CrossRef](#)] [[PubMed](#)]
77. Ott, V.L.; Cambier, J.C.; Kappler, J.; Marrack, P.; Swanson, B.J. Mast cell-dependent migration of effector CD8<sup>+</sup> T cells through production of leukotriene B<sub>4</sub>. *Nat. Immunol.* **2003**, *4*, 974–981. [[CrossRef](#)]
78. Kubes, P.; Ward, P.A. Leukocyte recruitment and the acute inflammatory response. *Brain Pathol.* **2000**, *10*, 127–135. [[CrossRef](#)]
79. Verma, V.; Sheikh, Z.; Ahmed, A.S. Nociception and role of immune system in pain. *Acta Neurol. Belg.* **2015**, *115*, 213–220. [[CrossRef](#)]
80. Andreacos, E.; Papadaki, M.; Serhan, C.N. Dexamethasone, pro-resolving lipid mediators and resolution of inflammation in COVID-19. *Allergy Eur. J. Allergy Clin. Immunol.* **2021**, *76*, 626–628. [[CrossRef](#)] [[PubMed](#)]
81. Schloer, S.; Pajonczyk, D.; Rescher, U. Annexins in translational research: Hidden treasures to be found. *Int. J. Mol. Sci.* **2018**, *19*, 1781. [[CrossRef](#)]
82. Yang, Y.H.; Morand, E.F.; Getting, S.J.; Paul-Clark, M.; Liu, D.L.; Yona, S.; Hannon, R.; Buckingham, J.C.; Perretti, M.; Flower, R.J. Modulation of Inflammation and Response to Dexamethasone by Annexin 1 in Antigen-Induced Arthritis. *Arthritis Rheum.* **2004**, *50*, 976–984. [[CrossRef](#)] [[PubMed](#)]
83. Hannon, R.; Croxtall, J.D.; Getting, S.J.; Roviezzo, F.; Yona, S.; Paul-Clark, M.J.; Gavins, F.N.E.; Perretti, M.; Morris, J.F.; Buckingham, J.C.; et al. Aberrant inflammation and resistance to glucocorticoids in annexin 1<sup>-/-</sup> mouse. *FASEB J.* **2003**, *17*, 253–255. [[CrossRef](#)] [[PubMed](#)]
84. Pupjalis, D.; Goetsch, J.; Kottas, D.J.; Gerke, V.; Rescher, U. Annexin A1 released from apoptotic cells acts through formyl peptide receptors to dampen inflammatory monocyte activation via JAK/STAT/SOCS signalling. *EMBO Mol. Med.* **2011**, *3*, 102–114. [[CrossRef](#)] [[PubMed](#)]
85. Gobbetti, T.; Cooray, S.N. Annexin A1 and resolution of inflammation: Tissue repairing properties and signalling signature. *Biol. Chem.* **2016**, *397*, 981–993. [[CrossRef](#)] [[PubMed](#)]